

A molecular dynamics study of the equation of state and the structure of supercooled aqueous solutions of methanol

Dario Corradini,^{1,a)} Zhiqiang Su,¹ H. Eugene Stanley,¹ and Paola Gallo²

¹Center for Polymer Studies and Department of Physics, Boston University, 590 Commonwealth Avenue, Boston, Massachusetts 02215, USA

²Dipartimento di Fisica, Università Roma Tre, Via della Vasca Navale 84, I-00146 Roma, Italy

(Received 10 August 2012; accepted 29 October 2012; published online 9 November 2012)

We perform molecular dynamics computer simulations in order to study the equation of state and the structure of supercooled aqueous solutions of methanol at methanol mole fractions $x_m = 0.05$ and $x_m = 0.10$. We model the solvent using the TIP4P/2005 potential and the methanol using the OPLS-AA force field. We find that for $x_m = 0.05$ the behavior of the equation of state, studied in the $P - T$ and $P - \rho$ planes, is consistent with the presence of a liquid-liquid phase transition, reminiscent of that previously found for $x_m = 0$. We estimate the position of the liquid-liquid critical point to be at $T = 193$ K, $P = 96$ MPa, and $\rho = 1.003$ g/cm³. When the methanol mole fraction is doubled to $x_m = 0.10$ no liquid-liquid transition is observed, indicating its possible disappearance at this concentration. We also study the water-water and water-methanol structure in the two solutions. We find that down to low temperature methanol can be incorporated into the water structure for both $x_m = 0.05$ and $x_m = 0.10$. © 2012 American Institute of Physics. [<http://dx.doi.org/10.1063/1.4767060>]

I. INTRODUCTION

Although water is the most common liquid in the natural world,¹ its complex behavior continues to fascinate both experimental and theoretical researchers.^{2–5} When compared to most other liquids, the thermodynamic properties of water are anomalous. Among the best-known water anomalies are: (i) the density anomaly, i.e., its density decreases upon isobaric cooling below the density maximum ($T = 277$ K at $P = 1$ atm), and (ii) its isobaric specific heat and the isothermal compressibility increase upon supercooling.⁶ Water also exhibits a large number of thermodynamic, structural, and dynamic anomalies.⁷

Many water anomalies are found in the metastable supercooled region.⁸ Over the past 20 years, several hypotheses have been proposed to explain the complex phenomenology of water^{2,3,5} in this region. The *liquid-liquid critical point* (LLCP) hypothesis⁹ ascribes the apparent divergent behavior of the thermodynamic response functions to the presence of a first-order liquid-liquid transition between a high density liquid (HDL) and a low density liquid (LDL), terminating at a LLCP. In the *singularity free* scenario,¹⁰ local density fluctuations determine the anomalous behavior of water, without the presence of a first-order liquid-liquid transition. The *critical point free* hypothesis¹¹ sees the liquid-liquid transition as an order-disorder transition with no critical point.

At present no consensus exists on the origin of the anomalies of water because the experimental investigation of the deep supercooled region is hampered by the presence of a homogeneous nucleation line ($T_H \simeq 235$ K at $P = 1$ atm).^{3,8} However, measurements of the decompression-induced melting line of ice IV¹² and extrapolations of the equation of state

(EOS) of supercooled water¹³ are consistent with the existence of a LLCP at $T_c \approx 220$ K and $P_c \approx 50$ – 100 MPa. Recent experimental evidence also signaled the presence of a liquid-liquid transition in water confined in MCM-41 cylindrical pores.^{14–16}

Computational studies have also found a liquid-liquid transition in bulk water. “All-atom” models, such as ST2,^{9,17–22} TIP4P,²³ TIP4P-Ew,²⁴ TIP4P/2005,²⁵ TIP5P,²⁶ and TIP5P-E,²⁷ display in their supercooled region a liquid-liquid transition and a LLCP. A second critical point was also observed in coarse-grained models for water, such as the Jagla model, an isotropic monoatomic model,^{28–31} and in 2D lattice models.³² Computer simulations also show the presence of an ideal extension of the liquid-liquid coexistence line in the one phase region, the Widom line, along which the thermodynamic response functions show extrema.^{28,33,34}

The complex phenomenology of supercooled bulk water has recently stimulated a vivid interest in the properties of supercooled aqueous solutions.^{23,35–49} On the one hand, the study of aqueous solutions can help to shed light on the open questions concerning bulk water, both from an experimental and a theoretical perspective. On the other hand aqueous solutions are interesting *per se*, given their ubiquitous presence in science, engineering, and industry.

A LLCP was found in molecular dynamics (MD) simulations on solutions of hydrophilic ionic solutes, namely, NaCl, in TIP4P water^{23,38} and it was shown that its position shifts towards higher temperatures and lower pressures upon increasing the solute content. The liquid-liquid critical properties of solutions of hydrophobic apolar solutes have been also studied with theoretical models³⁵ and discrete molecular dynamics simulations on hard spheres immersed in the Jagla solvent.^{23,50} Recently, an experiment on mixtures of water and glycerol⁴⁹ found evidence of a liquid-liquid transition possibly driven by the HDL-LDL transition of the solvent.

^{a)}darcorr@buphy.bu.edu.

Here, we study the thermodynamics and the structure of solutions of methanol in water, with methanol mole fractions $x_m = 0.05$ and $x_m = 0.10$ upon supercooling. We model the solvent using the TIP4P/2005 model⁵¹ and methanol using the OPLS-AA force field. The question of how the presence of methanol affects the liquid-liquid transition of water is interesting in more ways than one. Methanol is one of the simplest organic molecules and is thus a good candidate as a starting point for the study of solutions of water and biomolecules. Furthermore, methanol is an amphiphilic molecule composed of the hydrophobic methyl group, CH₃, and the hydrophilic “water-like” hydroxyl group, OH. Knowing the effect of an amphiphilic solute on the liquid-liquid properties of water is important for understanding the effects of different kinds of solute.

The paper is organized as follows. The details of the simulations performed are described in Sec. II. The results on the thermodynamics of the systems are presented in Sec. III, while those on the structural properties are presented in Sec. IV. Finally, conclusions are presented in Sec. V.

II. SIMULATION DETAILS

We perform MD all-atom simulations on two solutions of methanol in water. We fix the total number of particles in the cubic simulation box at $N = 1024$, and choose methanol mole fractions $x_m = 0.05$ and $x_m = 0.10$, the first corresponding to a methanol-water ratio of 1:19 (total 51:973) and the second to a ratio of 1:9 (total 102:922). The simulations are performed in the canonical NVT ensemble, changing the box length to select the desired density and using the Berendsen thermostat⁵² to adjust the temperature.

We model the solvent, water, using the TIP4P/2005 potential,⁵¹ the reparametrization by Abascal and Vega of the original TIP4P potential by Jorgensen *et al.*⁵³ This potential is the best non-polarizable rigid potential available for reproducing many features of experimental water.^{54–56} We model the solute, methanol, using the all-atom OPLS-AA potential for organic liquids.⁵⁷ This is a well-established model for methanol and it has been widely used in the literature on simulations of aqueous mixtures.^{58–63} It reproduces well the thermodynamic experimental behavior of methanol. The OPLS force field also reproduces the solid-solid and solid-fluid equilibria of pure methanol.^{64,65}

We employ a simulation time step of 1 fs for the Verlet leap-frog algorithm, and we cut off the short range Lennard-Jones portion of the interaction potential at 10 Å. We use the particle-mesh Ewald method to deal with the electrostatics, and we apply periodic boundary conditions. We use the software package GROMACS 4.5.3⁶⁶ to carry out the simulations.

We equilibrate the systems at $T = 500$ K and at $T = 400$ K to randomize the initial positions. From high temperature, $T = 350$ K, to low temperature, $T = 190$ K, the equilibration run is followed by a production run during which we record the thermodynamic quantities. We use the final configuration of one temperature as the initial configuration for the lower temperature, with $\Delta T = 5$ K. We progressively increase the equilibration and production times upon lowering the temperature, their sum ranging from 0.4 ns at ambient temperature to 25 ns

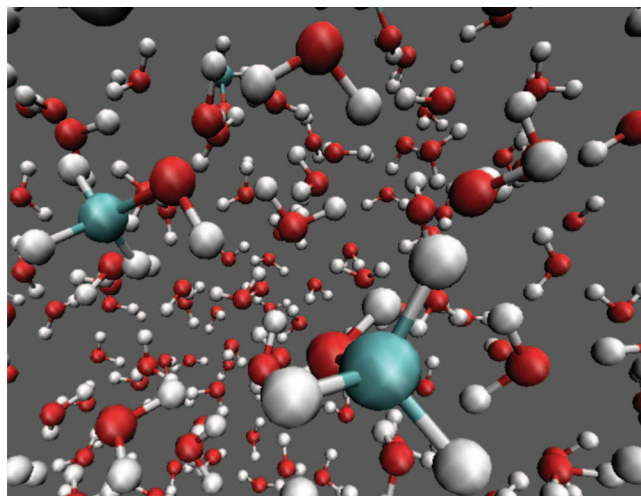


FIG. 1. Detail of two methanol molecules immersed in water taken from a blown-up snapshot of the $x_m = 0.10$ solution. For visualization purposes, only the atoms within a cube of 20 Å edge length in the center of the box are displayed. Atom color coding is: oxygen (red), hydrogen (white), and carbon (turquoise).

at the lowest temperature. The execution of the simulations required approximately 4 years of single core central processing unit time (AMD Athlon 3.1 GHz). The simulated densities span from $\rho = 1.10$ g/cm³ to $\rho = 0.94$ g/cm³ for the $x_m = 0.05$ solution and from $\rho = 1.10$ g/cm³ to $\rho = 0.92$ g/cm³ for the $x_m = 0.10$ solution. In the $x_m = 0.05$ case, we simulate three additional densities: $\rho = 1.015$ g/cm³, $\rho = 1.005$ g/cm³, and $\rho = 0.995$ g/cm³. To compare the structure, we also simulate TIP4P/2005 bulk water at $\rho = 1.10$ g/cm³, $\rho = 1.00$ g/cm³, and $\rho = 0.95$ g/cm³. The simulation conditions in bulk water are identical to the simulation conditions in the solutions and the number of water molecules considered is $N_{bulk} = 1024$.

Figure 1 shows a detail of two methanol molecules immersed in water taken from the magnified snapshot of the simulation box of the $x_m = 0.10$ solution.

III. THERMODYNAMIC RESULTS

There is a wide qualitative variety of phase equilibria in solutions. In fluid mixtures, lines of critical points can, depending on the features of the two components, emanate from the critical points of the pure substances (e.g., liquid-gas critical lines) but there can also be new critical phenomena associated with liquid-liquid demixing transitions.^{67,68} Demixing transitions are driven by a mechanism that differs from the mechanism that causes the “liquid-liquid transition” in pure water. In demixing transitions, the liquids forming the mixture are separated. In water liquid-liquid transition, there are two structural forms of the same liquid, HDL and LDL. The LLC in water is in fact of the same type as the liquid-gas critical point.^{22,31} Usually, one can distinguish between mechanical instabilities associated with the divergence of the correlation length of density fluctuations, and material instabilities associated with the divergence of the correlation length of concentration fluctuations.⁶⁷

In our case, where only one of the two substances (water) has a LLC, we expect only one critical line close to

the location of the solvent LLCP. Therefore, there can be only one HDL-LDL like critical point for each mole fraction of methanol in water. The LLCP for a given composition can be found spanning the whole $P - T$ (or $P - \rho$) diagram keeping the composition fixed. For our critical phenomenon in fact, similar to the liquid-gas critical point in solutions, the relevant fluctuations are those of the density of the solvent between LDL and HDL upon approaching the LLCP. Thus, the behavior in the $P - T$ or $P - \rho$ space will be similar to that of the pure substance until the phenomenon can persist. The increase of the solute concentration above a certain edge could perturb the water molecules behavior and cause the LLCP to disappear. See, for example, how water anomalies disappear as salt is added above a certain level.^{69,70}

In aqueous solutions of methanol or other aliphatic alcohols, experimental $P - T$ and $P - \rho$ diagrams indicate the location of the liquid-gas critical point of the mixture⁷¹⁻⁷³ and display a phenomenology akin to the liquid-gas transition of pure water.

In this section, we present the results on the thermodynamics obtained from our MD simulations for the $x_m = 0.05$ and $x_m = 0.10$ solutions of methanol in TIP4P/2005 water. Figure 2 shows the EOS in the $P - T$ isochores plane of the $x_m = 0.05$ solution of methanol in water. The isochores displayed range from $\rho = 0.94 \text{ g/cm}^3$ to $\rho = 1.10 \text{ g/cm}^3$. We fit the simulated state points to a fourth-degree polynomial function.

All the isochores but the one of highest density, $\rho = 1.10 \text{ g/cm}^3$, show a minimum in the spanned range of temperatures. A minimum in the isochores indicates the onset of the region of density anomaly, where the density of the system decreases upon isobaric cooling. The border of this region is the temperature of maximum density (TMD) line and its points can be extracted from the EOS looking at the minima of the isochores where the coefficient of thermal expansion $\alpha_P = -(\partial\rho/\partial T)_P/\rho$ equals 0.

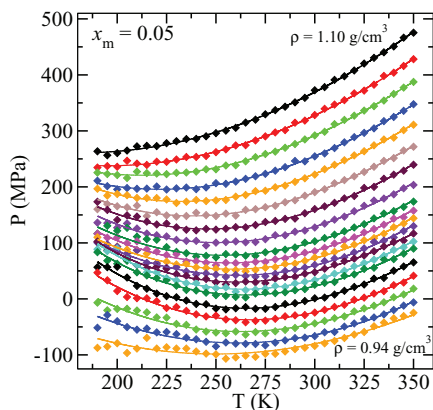


FIG. 2. EOS in the $P - T$ isochores plane of the $x_m = 0.05$ solution. The state points reported (diamonds) span temperatures from $T = 350 \text{ K}$ to $T = 190 \text{ K}$. The isochores shown are at densities, in g/cm^3 , $0.94 \leq \rho \leq 0.99$ every $\Delta\rho = 0.01$, $\rho = 0.995$, $\rho = 1.00$, $\rho = 1.005$, $\rho = 1.01$, $\rho = 1.015$, and $1.02 \leq \rho \leq 1.10$ every $\Delta\rho = 0.01$ (from bottom to top). The lines are fourth-degree polynomial fits to the simulated state points. The convergence of the isochores points to a LLCP located at $190 \text{ K} < T_c < 195 \text{ K}$, $90 \text{ MPa} < P_c < 100 \text{ MPa}$, and $1.00 \text{ g/cm}^3 < \rho_c < 1.005 \text{ g/cm}^3$.

In the central region of the spanned range of densities, the isochores at $\rho = 0.995 \text{ g/cm}^3$, $\rho = 1.00 \text{ g/cm}^3$, and $\rho = 1.005 \text{ g/cm}^3$ appear to converge at low temperature, between $T = 190 \text{ K}$ and $T = 195 \text{ K}$ and at a pressure between 90 MPa and 100 MPa . The highest point of convergence of the isochores corresponds to a horizontal inflection point of the isotherms, where $(\partial P/\partial\rho)_T = (\partial^2 P/\partial\rho^2)_T = 0$ and thus indicates the presence of a LLCP (see, for example, Refs. 19, 29, and 71-74).

To better determine the position of the LLCP of the $x_m = 0.05$ solution of methanol in water, we plot in Fig. 3 the simulated state points in the $P - \rho$ isotherms plane, together with the isotherms extracted from the fits of Fig. 2. The isotherms in the range $T = 190 \text{ K} - T = 220 \text{ K}$ are shown with higher temperature isotherms $T = 250 \text{ K}$, $T = 280 \text{ K}$, and $T = 300 \text{ K}$ reported for comparison. Note that a horizontal inflection point appears to emerge between the $T = 195 \text{ K}$ and the $T = 190 \text{ K}$ isotherms, at a density between $\rho = 1.00 \text{ g/cm}^3$ and $\rho = 1.005 \text{ g/cm}^3$. The plot of the isotherms allows us to assign critical parameters for the $x_m = 0.05$ solution at $T_c \simeq 193 \text{ K}$, $P_c \simeq 96 \text{ MPa}$, and $\rho_c \simeq 1.003 \text{ g/cm}^3$.

The inset of Fig. 3 shows the isobars from $P = 40 \text{ MPa}$ to $P = 97 \text{ MPa}$ extracted from the fits in Fig. 2. Vertical inflections begin to appear at $P = 50 \text{ MPa}$, become marked at $P = 70 \text{ MPa}$, and progressively more marked until a vertical inflection point develops between the $P = 95 \text{ MPa}$ and $P = 97 \text{ MPa}$ isobars. Studying the isobars confirms the critical parameters determined through the isotherms.

Abascal and Vega²⁵ studied the bulk TIP4P/2005 liquid-liquid critical properties and they found the critical parameters $T_c^{\text{Bulk}} = 193 \text{ K}$, $P_c^{\text{Bulk}} = 135 \text{ MPa}$, and $\rho_c^{\text{Bulk}} = 1.012 \text{ g/cm}^3$. These values are close to the ones determined for the original TIP4P potential by Corradini *et al.*,²³ namely, $T_c^{\text{Bulk}} = 190 \text{ K}$,

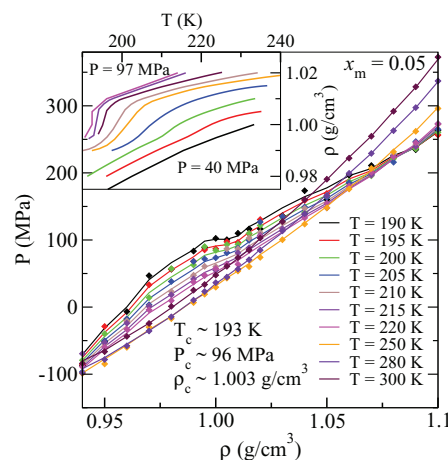


FIG. 3. EOS in the $P - \rho$ isotherms plane of the $x_m = 0.05$ solution. The state points (diamonds) are shown for temperatures $190 \text{ K} \leq T \leq 220 \text{ K}$ every $\Delta T = 5 \text{ K}$, $T = 250 \text{ K}$, $T = 280 \text{ K}$, and $T = 300 \text{ K}$. The lines are obtained from the polynomial fits shown in Fig. 2. A horizontal inflection point develops between the $T = 195 \text{ K}$ and the $T = 190 \text{ K}$ isotherms. (Inset) Isobars obtained performing horizontal cuts on the polynomial fits shown in Fig. 2 for pressures, in MPa, $P = 40, 50, 60, 70, 80, 85, 91.5, 95, 97$ (from bottom to top). A vertical inflection point is observed between the $P = 95 \text{ MPa}$ and $P = 97 \text{ MPa}$ isobars. The behavior of the isotherms and the isobars is consistent with a LLCP at $T_c \simeq 193 \text{ K}$, $P_c \simeq 96 \text{ MPa}$, and $\rho_c \simeq 1.003 \text{ g/cm}^3$.

$P_c^{\text{Bulk}} = 150$ MPa, and $\rho_c^{\text{Bulk}} = 1.06$ g/cm³. Therefore, we find that at $x_m = 0.05$ methanol mole fraction, the critical properties remain very similar to those of bulk water. In fact the critical temperature is the same, while the critical density is slightly lower in the solution case. In contrast to the bulk case, in the $x_m = 0.05$ solution the critical pressure decreases by about 40 MPa, and this fact could simplify the experimental determination of the LLCP in water-methanol mixtures. Recently, on the basis of experimental data, the critical pressure in aqueous solutions of glycerol⁴⁹ was inferred to shift downwards upon increasing the solute concentration. Because glycerol is an amphiphilic molecule like methanol, this fact appears consistent with the shift in pressure we find.

It was previously noted for other mixtures and for confined water^{23,38,39,75–79} that the region within which phenomena associated with the liquid-liquid transition can be observed is smaller than in bulk water. In our case, the vertical inflections in the isobars corresponding to the Widom line are visible from approximately $P = 50$ MPa to the critical pressure $P = 96$ MPa. In bulk TIP4P/2005 water, they are visible across a much wider span of pressures, from 0.1 to 150 MPa.²⁵

We next study the effect of doubling the concentration of methanol on the EOS. Figure 4 shows a plot in the $P - T$ isochores plane of the simulated state points for the $x_m = 0.10$ solution of methanol in water. The isochores shown span densities from $\rho = 0.92$ g/cm³ to $\rho = 1.10$ g/cm³ and are again fitted to fourth-degree polynomial functions. At this methanol mole fraction, we find that the isochore minima are confined to a range of $\rho = 1.06$ g/cm³ to $\rho = 0.94$ g/cm³, and that they are always at a lower temperature than in the $x_m = 0.05$ case. Note that the isochores do not converge when $x_m = 0.10$. Although this may imply that the LLCP has disappeared at this concentration, it does not rule out the possibility that it may be found at a lower temperature outside the spanned range of the simulation. At $x_m = 0.05$, the Widom line region seems to be much smaller than in the bulk case, so it is possible that a further increase in the concentration could wash away

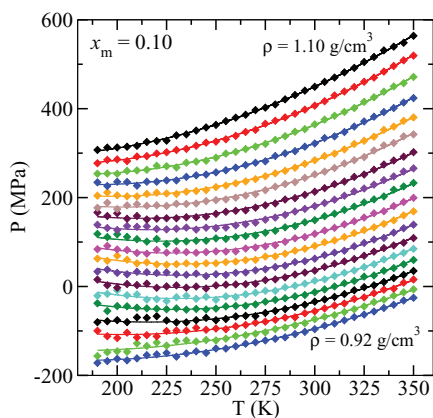


FIG. 4. EOS in the $P - T$ isochores plane of the $x_m = 0.10$ solution. The state points reported (diamonds) span temperatures from $T = 350$ K to $T = 190$ K. The isochores shown are at densities, in g/cm³, $0.92 \leq \rho \leq 1.10$ every $\Delta\rho = 0.01$ (from bottom to top). The lines are fourth-degree polynomial fits to the simulated state points. No point of convergence of the isochores is observed in the spanned region.

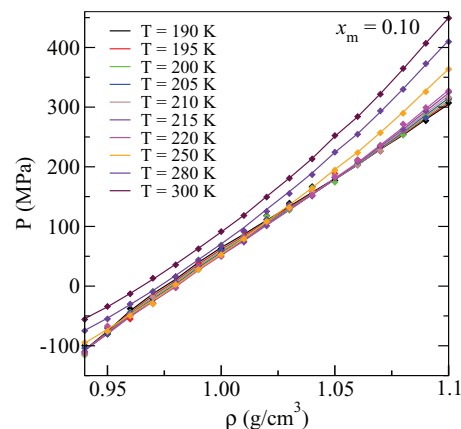


FIG. 5. EOS in the $P - \rho$ isotherms plane of the $x_m = 0.10$ solution. The state points (diamonds) are shown for temperatures $190 \text{ K} \leq T \leq 220 \text{ K}$ every $\Delta T = 5 \text{ K}$, $T = 250 \text{ K}$, $T = 280 \text{ K}$, and $T = 300 \text{ K}$. The lines are obtained from the polynomial fits shown in Fig. 4.

the liquid-liquid transition. In aqueous solutions of salts it has been found experimentally that the anomalous behavior of the thermodynamic response functions is progressively lost when the concentration of solutes is increased.^{69,70}

Figure 5 shows the simulated state points for the $x_m = 0.10$ solution in the $P - \rho$ isotherms plane together with the isotherms obtained from the fits in Fig. 4. Comparing the isotherms of the $x_m = 0.10$ solution with the isotherms of the $x_m = 0.05$ solution (see Fig. 3), we see that there is no evidence of an inflection point and thus of a LLCP in the isotherms of the $x_m = 0.10$ solution. This confirms what is shown in Fig. 4.

Figure 6 shows the LLCP found for the $x_m = 0.05$ solution (see Figs. 2 and 3) in the $P - T$ phase diagram, and compares it with the LLCP of bulk TIP4P/2005 water.²⁵ It shows the minima of the coefficient of thermal expansion α_P (see also the inset of Fig. 3) and the maxima of the isothermal compressibility $K_T = (\partial\rho/\partial P)_T/\rho$ calculated from the simulated state points close to the LLCP of the $x_m = 0.05$ solution. It also shows the TMD points determined from the simulated state points of the $x_m = 0.05$ solution (see Fig. 2) and $x_m = 0.10$ solution (see Fig. 4), and compares them with the TMD line of bulk TIP4P/2005 water.^{25,56}

In the $P - T$ plane, the LLCP of the $x_m = 0.05$ solution falls very close to the LLCP of bulk TIP4P/2005 water, although it is significant that it is found at a lower pressure, $\Delta P_c \equiv P_c^{\text{sol}} - P_c^{\text{Bulk}} \simeq -40$ MPa. Figure 6 shows that the line of the isothermal compressibility maxima calculated along the isotherms and the line of the coefficient of thermal expansion minima calculated along the isobars (shown in the inset of Fig. 3) fall very close to each other, forming the Widom line in the one phase region close to the LLCP of the $x_m = 0.05$ solution.

The TMD points have been determined from the minima of the isochores of the $x_m = 0.05$ and the $x_m = 0.10$ solutions. Note that when the concentration of methanol increases, the TMD shifts to lower temperatures. At higher pressures the TMD in the $x_m = 0.05$ solution is similar to the TMD in bulk water, albeit at slightly lower temperatures, and at lower pressures it shifts to markedly lower temperatures. In contrast, the

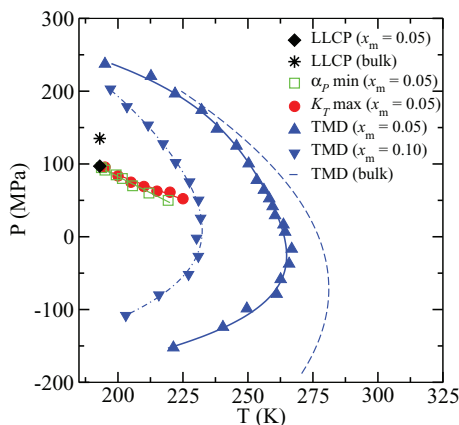


FIG. 6. Shown is the position of the LLCP in the $x_m = 0.05$ solution (diamond), estimated using Figs. 2 and 3, compared to the LLCP in TIP4P/2005 bulk water (star).²⁵ The line of extrema of the coefficient of thermal expansion α_P (squares) and of the isothermal compressibility K_T (circles) converge at the LLCP. The TMD points calculated for $x_m = 0.05$ (triangles up) and $x_m = 0.10$ (triangles down) are also compared with the TMD line of TIP4P/2005 bulk water obtained by fitting the points calculated in Refs. 25 and 56 (dashed line).

TMD of the $x_m = 0.10$ solution is always found at temperatures significantly lower than the TMD of bulk water. For a quantitative comparison, we measure the TMD shift at atmospheric pressure $P_{\text{atm}} = 0.1$ MPa. For the $x_m = 0.05$ solution $\Delta T_{\text{atm}}^{\text{TMD}} \equiv T_{\text{atm}}^{\text{sol}} - T_{\text{atm}}^{\text{Bulk}} \simeq -13$ K, while for the $x_m = 0.10$ solution $\Delta T_{\text{atm}}^{\text{TMD}} \simeq -45$ K. Note that the direction of the shift in the TMD when the concentration of methanol is increased is in accord with experimental,⁸⁰ theoretical,⁸¹ and computer simulation⁸² results.

IV. STRUCTURAL RESULTS

In this section, we present our calculations on the structure of the $x_m = 0.05$ and the $x_m = 0.10$ solutions of methanol in water, and we compare them with our calculations on the structure of bulk TIP4P/2005 water.

We first focus on the water oxygen-water oxygen (Ow–Ow) radial distribution functions (RDFs). The characteristics of the HDL and LDL Ow–Ow RDFs were previously described in the literature (see, for example, Refs. 83–86). The shape of the first peak of the Ow–Ow RDF in HDL and LDL is similar, but the height is slightly higher in LDL. The nature of the liquid is determined mostly by the shape of the second shell. The second peak of LDL is very pronounced with a corresponding deep first minimum between the first and second shells. On the other hand, in HDL the second peak is shifted to lower distances and it is not as high as in LDL, with a shallower minimum between the first and second shells. This is similar to what happens to water under pressure or in confinement.⁸⁷

Figure 7 shows the Ow–Ow radial distribution functions for three systems—bulk TIP4P/2005 water, the $x_m = 0.05$ solution, and the $x_m = 0.10$ solution—at three densities: $\rho = 1.10$ g/cm³, $\rho = 1.00$ g/cm³, and $\rho = 0.95$ g/cm³. We display the RDFs at $T = 190$ K, a temperature immediately below the estimated LLCP of bulk water and of the $x_m = 0.05$

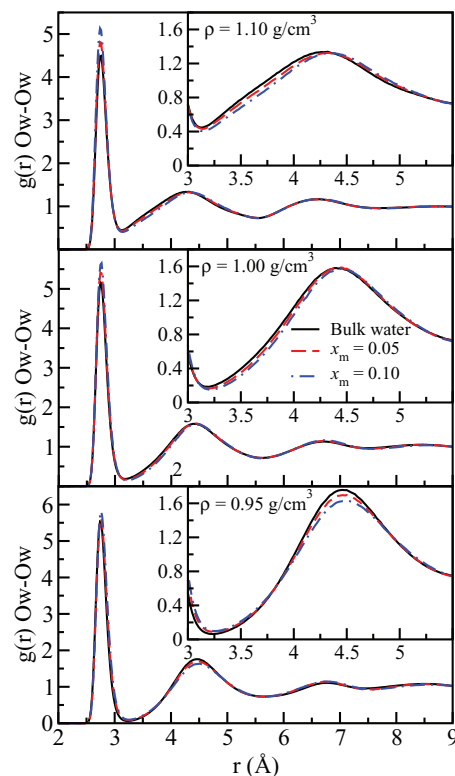


FIG. 7. Water oxygen-water oxygen (Ow–Ow) RDFs at $T = 190$ K and at $\rho = 1.10$ g/cm³ (top), $\rho = 1.00$ g/cm³ (middle), and $\rho = 0.95$ g/cm³ (bottom) for bulk water (solid line), and the $x_m = 0.05$ (dashed line) and $x_m = 0.10$ (dotted-dashed line) solutions. The insets show a magnification of the region close to the second shell.

solution. The insets are a blow-up of the region close to the second peak of the RDF.

We see that the Ow–Ow structure in the solutions is similar to that of bulk water at all densities. Experimental results have shown that the solutes have a much more dramatic effect on water-water structure when the solution has a higher methanol content, $x_m = 0.27$ and $x_m = 0.54$.⁸⁸ Note that at $\rho = 0.95$ g/cm³, the three systems exhibit LDL characteristics, with second peak positions from 4.46 to 4.49 Å (going from bulk to the $x_m = 0.10$ solution) and corresponding heights from 1.75 to 1.61. At $\rho = 1.10$ g/cm³, they show HDL characteristics with second peak positions from 4.29 to 4.35 Å and heights from 1.34 to 1.33. Thus when $x_m = 0.10$, despite the apparent lack of a first-order phase transition, there is still a gradual transformation between the two liquids. The $\rho = 1.00$ g/cm³ case appears to be intermediate between HDL and LDL, with positions of the second peak (always from bulk to the $x_m = 0.10$ solution) from 4.41 Å to 4.45 Å and corresponding heights from 1.57 to 1.56.

The overall shape of the Ow–Ow RDFs remains similar to that in bulk water when the methanol mole fraction is increased, although for the LDL case the effect is larger. In fact, in the solutions the positions of maxima and minima of the RDFs are similar to those in bulk water, but a slight reduction in the height of the second peak can be seen in LDL when the concentration of methanol is increased. The second peak height is 1.75 in bulk TIP4P/2005 water, 1.69 in the $x_m = 0.05$ solution, and 1.61 in the $x_m = 0.10$ solution. This

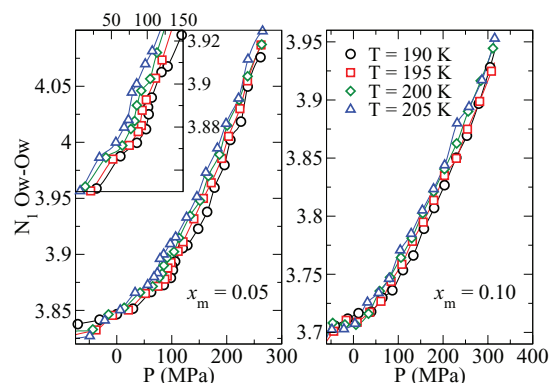


FIG. 8. Ow–Ow first shell coordination numbers N_1 calculated integrating the RDFs up to $r = 3.2$ Å as a function of pressure for the $x_m = 0.05$ (left) and $x_m = 0.10$ (right) solutions. The temperatures shown are $T = 190$ K, $T = 195$ K, $T = 200$ K, and $T = 205$ K. The inset of the left panel shows a magnification of the region close to the LLCP of the $x_m = 0.05$ solution.

slight reduction in the LDL character of the Ow–Ow RDF is consistent with the downward shift of the critical pressure in the $x_m = 0.05$ with respect to the bulk (see Fig. 6), indicating a stabilization of the HDL phase when methanol is present. It was previously observed that salts, e.g., NaCl, have a stronger effect in modifying LDL water structure, rendering it more similar to HDL water structure.^{85,86}

We have seen that both the $x_m = 0.05$ and $x_m = 0.10$ solutions show an Ow–Ow RDF with HDL characteristics at high density and an Ow–Ow RDF with LDL characteristics at low density, despite the fact that the $x_m = 0.05$ shows a LLCP and the $x_m = 0.10$ does not. Here, we study how the first water shell changes with pressure. We look at the Ow–Ow first shell coordination numbers N_1 , i.e., the number of water molecules contained in the first shell around a central molecule. Figure 8 shows the behavior of N_1 as a function of pressure for the $x_m = 0.05$ (left panel) and the $x_m = 0.10$ (right panel) solutions. We report the values for the four lowest temperatures simulated, $T = 205$ K, $T = 200$ K, $T = 195$ K, and $T = 190$ K.

In both cases $N_1 \approx 4$, even at high pressures, which is a typical value of LDL. It decreases even further at low pressures, where LDL is expected. This reduction of the N_1 is likely due to the O–H groups in methanol taking the place of the O–H groups in water in some of the water hydration shells.

For $x_m = 0.10$, the trend of the first shell coordination numbers changes smoothly with pressure, but an almost vertical inflection is found for the $x_m = 0.05$ solution at pressures around 100 MPa. This fact is consistent with the presence of a first-order liquid-liquid transition in the $x_m = 0.05$ solution, and its absence in the $x_m = 0.10$ case. A vertical inflection in the behavior of the first shell coordination numbers as a function of pressure was observed for supercooled liquid silicon, corresponding to a liquid-liquid transition.⁸⁹

Finally, in order to compare this with the Ow–Ow structure, Fig. 9 shows the water oxygen-methanol oxygen (Ow–Om) RDFs for the $x_m = 0.05$ and the $x_m = 0.10$ solutions. As in the case of the Ow–Ow RDFs, the results are shown at $T = 190$ K and for densities $\rho = 1.10$ g/cm³, $\rho = 1.00$ g/cm³, and $\rho = 0.95$ g/cm³. We also show the bulk Ow–Ow RDFs

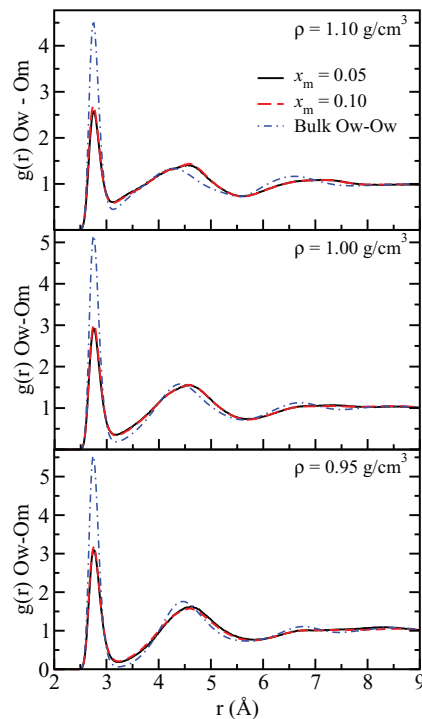


FIG. 9. Water oxygen–methanol oxygen (Ow–Om) RDFs at $T = 190$ K and at $\rho = 1.10$ g/cm³ (top), $\rho = 1.00$ g/cm³ (middle), and $\rho = 0.95$ g/cm³ (bottom) for the $x_m = 0.05$ (solid line) and $x_m = 0.10$ (dashed line) solutions. For comparison the bulk water oxygen–oxygen (Ow–Ow) RDFs (dotted-dashed lines) at the corresponding densities are also shown.

at the corresponding densities. The first peak of both Ow–Om and Ow–Ow falls at exactly the same position, indicating that the O–H of methanol can indeed be fit into the coordination structure of water, as previously hypothesized when looking at the Ow–Ow first shell coordination numbers. The fact that methanol can be fit into water structure with the oxygen of methanol replacing one oxygen of water in the water network is in agreement with experimental findings on the dynamics⁹⁰ and structure⁹¹ of solutions of methanol in water at ambient temperature and above. The second Ow–Om shell seems to still retain water-like characteristics but is shifted to a longer distance, probably due to the need to accommodate sterically the CH₃ group of methanol. At both high density and low density, the second peak of the Ow–Om is always found at approximately 4.6 Å. In the HDL the second shell is more dissimilar to the Ow–Ow case and assumes a strongly asymmetrical shape. The third shell appears at all densities to be only hinted when compared to the Ow–Ow case and it is always found at longer distances. Despite the noted differences, the Ow–Om remains overall similar to the water Ow–Ow structure and, when we go from the LDL to the HDL, we see that the Ow–Om structure shows changes similar to those of the Ow–Ow case, namely, the intensity of the first peak decreases and the second shell moves to shorter distances.

V. CONCLUSIONS

We perform all-atom MD simulations of two solutions of methanol in water, with methanol mole fraction $x_m = 0.05$ and $x_m = 0.10$, upon supercooling. The TIP4P/2005 model is

used for water and the OPLS-AA force field is employed for methanol. We study the EOS of the systems obtained from NVT simulations and the water-water and water-methanol structure in the two solutions.

A liquid-liquid phase transition ending in a LLCPC was observed in bulk TIP4P/2005.²⁵ We find that, for the $x_m = 0.05$ solution, we still see a LLCPC, its position being close to the one in bulk water but at a lower pressure. We estimate the position of the $x_m = 0.05$ solution LLCPC at $T = 193$ K, $P = 96$ MPa, and $\rho = 1.003$ g/cm³. Since the critical pressure estimated for bulk TIP4P/2005 is $P = 135$ MPa, we observe a shift of approximately -40 MPa in the critical pressure when going from bulk water to $x_m = 0.05$. This downward shift in pressure may ease the experimental determination of the LLCPC in mixtures of methanol and water, since the homogeneous nucleation temperature also shifts down significantly in an aqueous solution of methanol (approximately 7 K for $x_m = 0.05$).⁹²

The position of the LLCPC computed in simulations varies according to the force-field employed.²³ In bulk TIP4P, which has liquid-liquid critical parameters close to TIP4P/2005, we need to raise the temperatures and lower the pressures ($\Delta T = +31$ and $\Delta P = -73$ MPa) in its phase diagram to match the TMD and LLCPC values estimated in experiments.^{12,13} Thus finding a LLCPC in simulations of the $x_m = 0.05$ solution at the same temperature and at a lower pressure than in the bulk may have experimental relevance because:

- (i) the experimental critical temperature is probably higher than the critical temperature computed in simulations (as indicated by the results on TIP4P²³) and at the same time the homogeneous nucleation temperature shifts down in the solution,⁹² and
- (ii) the critical pressure decreases with respect to the bulk and approaches values closer to atmospheric pressure (even more when taking into account that the experimental critical pressure may be less than the critical pressure obtained in simulations).

The region where anomalies connected to the Widom line are present, in the one phase region above the LLCPC, appears narrower than in the bulk case, consistent with previous results for water in solutions or confinement.^{23,38,39,75-79}

A much more dramatic shift of the critical point towards higher temperature and lower (negative) pressure with respect to the bulk was previously observed in sodium chloride aqueous solutions,^{23,38} even at mole fractions much lower than $x = 0.05$. Thus, it appears that methanol exerts a much weaker effect than do ions on the critical properties of water.

When the mole fraction of methanol is doubled to $x_m = 0.10$, we find no indication that a liquid-liquid transition or a LLCPC is present. Although our calculations do not prove conclusively that such a transition does not occur at this methanol mole fraction, the progressive reduction of the region of anomalies associated with the LLCPC upon increasing concentration and the lack of a vertical inflection in the trend of the Ow–Ow coordination numbers versus pressure suggests that its disappearance is plausible.

We also study the water-water and water-methanol structure in our systems. We observe that the effect of the pres-

ence of methanol on the water-water RDFs is very mild and is slightly more significant in LDL water. We also see that when the Ow–Ow first shell coordination numbers are plotted against pressure they show a smooth trend at $x_m = 0.10$, where no transition occurs, but display a vertical inflection for pressures close to the LLCPC pressure of the $x_m = 0.05$ solution, confirming the results obtained studying the thermodynamics. The Ow–Om RDFs show that methanol can be readily incorporated into the structure of water. This “affinity” for water structure could be the reason the shift of the critical properties with respect to bulk properties is smaller than that caused by ions.

ACKNOWLEDGMENTS

D.C., Z.S., and H.E.S. thank the NSF Chemistry Division for support (Grant Nos. CHE 0911389, CHE 0908218, and CHE-1213217). P.G. gratefully acknowledges the computational support received by the INFN RM3-GRID at Roma Tre University.

¹F. Franks, *Water, A Matrix For Life*, 2nd ed. (Royal Society of Chemistry, Cambridge, England, 2000).

²P. G. Debenedetti and H. E. Stanley, *Phys. Today* **56**(6), 40 (2003).

³P. G. Debenedetti, *J. Phys.: Condens. Matter* **15**, R1669 (2003).

⁴A. Nilsson and L. G. M. Pettersson, *Chem. Phys.* **389**, 1 (2011).

⁵See, e.g., the review by F. Mallamace, *Liquid Polymorphism*, edited by H. E. Stanley, *Advances in Chemical Physics* Vol. 152 (Wiley, New York, 2012).

⁶R. J. Speedy and C. A. Angell, *J. Chem. Phys.* **65**, 851 (1976).

⁷J. R. Errington and P. G. Debenedetti, *Nature (London)* **409**, 318 (2001).

⁸P. G. Debenedetti, *Metastable Liquids: Concepts and Principles* (Princeton University, Princeton, NJ, 1996).

⁹P. H. Poole, F. Sciortino, U. Essmann, and H. E. Stanley, *Nature (London)* **360**, 324 (1992).

¹⁰S. Sastry, P. G. Debenedetti, F. Sciortino, and H. E. Stanley, *Phys. Rev. E* **53**, 6144 (1996); H. E. Stanley and J. Teixeira, *J. Chem. Phys.* **73**, 3404 (1980); H. E. Stanley, *J. Phys. A* **12**, L329 (1979).

¹¹C. A. Angell, *Science* **319**, 582 (2008).

¹²O. Mishima and H. E. Stanley, *Nature (London)* **392**, 164 (1998); **396**, 329 (1998).

¹³O. Mishima, *J. Chem. Phys.* **133**, 144503 (2010).

¹⁴Y. Zhang, A. Faraone, W. A. Kamitakahara, K.-H. Liu, C.-Y. Mou, J. B. Leão, S. Chang and S.-H. Chen, *Proc. Natl. Acad. Sci. U.S.A.* **108**, 12206 (2011).

¹⁵L. Liu, S.-H. Chen, A. Faraone, C.-W. Yen, and C.-Y. Mou, *Phys. Rev. Lett.* **95**, 117802 (2005).

¹⁶D. Liu, Y. Zhang, C.-C. Chen, C.-Y. Mou, P. H. Poole, and S.-H. Chen, *Proc. Natl. Acad. Sci. U.S.A.* **104**, 9570 (2007).

¹⁷P. H. Poole, F. Sciortino, U. Essmann, and H. E. Stanley, *Phys. Rev. E* **48**, 3799 (1993).

¹⁸F. Sciortino, P. H. Poole, U. Essmann, and H. E. Stanley, *Phys. Rev. E* **55**, 727 (1997).

¹⁹P. H. Poole, I. Saika-Voivod, and F. Sciortino, *J. Phys. Condens. Matter* **17**, L431 (2005).

²⁰Y. Liu, A. Z. Panagiotopoulos, and P. G. Debenedetti, *J. Chem. Phys.* **131**, 104508 (2009); Y. Liu, J. C. Palmer, A. Z. Panagiotopoulos, and P. G. Debenedetti, “Liquid-liquid transition in ST2 water,” *J. Chem. Phys.* (submitted).

²¹F. Sciortino, I. Saika-Voivod, and P. H. Poole, *Phys. Chem. Chem. Phys.* **13**, 19759 (2011); P. H. Poole, S. R. Becker, F. Sciortino, and F. W. Starr, *J. Phys. Chem. B* **115**, 14176 (2011).

²²T. A. Kesselring, G. Franzese, S. V. Buldyrev, H. J. Herrmann, and H. E. Stanley, *Sci. Rep.* **2**, 474 (2012); E. Lascaris *et al.*, “Finite size analysis of the hypothesized critical point in supercooled water,” *J. Chem. Phys.* (submitted).

²³D. Corradini, M. Rovere, and P. Gallo, *J. Chem. Phys.* **132**, 134508 (2010).

²⁴D. Paschek, A. Ruppert, and A. Geiger, *Chem. Phys. Chem.* **9**, 2737 (2008).

- ²⁵J. L. F. Abascal and C. Vega, *J. Chem. Phys.* **133**, 234502 (2010); **134**, 186101 (2011).
- ²⁶M. Yamada, S. Mossa, H. E. Stanley, and F. Sciortino, *Phys. Rev. Lett.* **88**, 195701 (2002).
- ²⁷D. Paschek, *Phys. Rev. Lett.* **94**, 217802 (2005).
- ²⁸L. Xu, P. Kumar, S. V. Buldyrev, S.-H. Chen, P. H. Poole, F. Sciortino, and H. E. Stanley, *Proc. Natl. Acad. Sci. U.S.A.* **102**, 16558 (2005).
- ²⁹L. Xu, S. V. Buldyrev, C. A. Angell, and H. E. Stanley, *Phys. Rev. E* **74**, 031108 (2006).
- ³⁰J. Y. Abraham, S. V. Buldyrev, and N. Giovambattista, *J. Phys. Chem. B* **115**, 48 (2011).
- ³¹P. Gallo and F. Sciortino, *Phys. Rev. Lett.* **109**, 177801 (2012).
- ³²K. Stokely, M. G. Mazza, H. E. Stanley, and G. Franzese, *Proc. Natl. Acad. Sci. U.S.A.* **107**, 1301 (2010); K. Stokely, H. E. Stanley, and G. Franzese, "A general theory of the thermodynamics of water and other network forming liquids," *J. Chem. Phys.* (submitted).
- ³³G. Franzese and H. E. Stanley, *J. Phys. Condens. Matter* **19**, 205126 (2007).
- ³⁴L. Xu, F. Mallamace, Z. Yan, F. W. Starr, S. V. Buldyrev, and H. E. Stanley, *Nat. Phys.* **5**, 565 (2009).
- ³⁵S. Chatterjee and P. G. Debenedetti, *J. Chem. Phys.* **124**, 154503 (2006).
- ³⁶D. Corradini, P. Gallo, and M. Rovere, *J. Chem. Phys.* **128**, 244508 (2008); **130**, 154511 (2009).
- ³⁷D. Corradini, P. Gallo, and M. Rovere, *J. Phys. Condens. Matter* **22**, 284104 (2010).
- ³⁸D. Corradini and P. Gallo, *J. Phys. Chem. B* **115**, 14161 (2011).
- ³⁹D. Corradini, S. V. Buldyrev, P. Gallo, and H. E. Stanley, *Phys. Rev. E* **81**, 061504 (2010).
- ⁴⁰F. Mallamace, C. Branca, C. Corsaro, N. Leone, J. Spooren, H. E. Stanley, and S.-H. Chen, *J. Phys. Chem. B* **114**, 1870 (2010).
- ⁴¹O. Mishima, *J. Chem. Phys.* **123**, 154506 (2005); **126**, 244507 (2007).
- ⁴²O. Mishima, *J. Phys. Chem. B* **115**, 14064 (2011).
- ⁴³L. Le and V. Molinero, *J. Chem. Phys. A* **115**, 5900 (2011).
- ⁴⁴C. Huang, T. M. Weiss, D. Nordlund, K. T. Wikfeldt, L. G. M. Pettersson, and A. Nilsson, *J. Chem. Phys.* **133**, 134504 (2010).
- ⁴⁵J. Holzmann, R. Ludwig, A. Geiger, and D. Paschek, *Chem. Phys. Chem.* **9**, 2722 (2008).
- ⁴⁶M. P. Longinotti, M. A. Carignano, I. Szleifer, and H. R. Corti, *J. Chem. Phys.* **134**, 244510 (2011).
- ⁴⁷H. R. Corti, F. J. Nores-Pondal, and C. A. Angell, *Phys. Chem. Chem. Phys.* **13**, 19741 (2011).
- ⁴⁸C. Corsaro, J. Spooren, C. Branca, N. Leone, M. Broccio, C. Kim, S.-H. Chen, H. E. Stanley, and F. Mallamace, *J. Chem. Phys.* **112**, 10449 (2008).
- ⁴⁹K. Murata and H. Tanaka, *Nature Mater.* **11**, 436 (2012).
- ⁵⁰D. Corradini, P. Gallo, S. V. Buldyrev, and H. E. Stanley, *Phys. Rev. E* **85**, 051503 (2012).
- ⁵¹J. L. F. Abascal and C. Vega, *J. Chem. Phys.* **123**, 234505 (2005).
- ⁵²H. J. C. Berendsen, J. P. M. Postma, W. F. van Gunsteren, A. DiNola, and J. R. Haak, *J. Chem. Phys.* **81**, 3684 (1984).
- ⁵³W. L. Jorgensen, J. Chandrasekhar, J. D. Madura, R. W. Impey, and M. L. Klein, *J. Chem. Phys.* **79**, 926 (1983).
- ⁵⁴C. Vega, J. L. F. Abascal, M. M. Conde, and J. L. Aragonés, *Faraday Discuss.* **141**, 251 (2009).
- ⁵⁵C. Vega and J. L. F. Abascal, *Phys. Chem. Chem. Phys.* **13**, 19663 (2011).
- ⁵⁶M. Agarwal, M. P. Alam, and C. Chakravarty, *J. Phys. Chem. B* **115**, 6935 (2011).
- ⁵⁷W. L. Jorgensen, D. S. Maxwell, and J. Tirado-Rives, *J. Am. Chem. Soc.* **118**, 11225 (1996).
- ⁵⁸J. Dai, X. Li, L. Zhao, and H. Sun, *Fluid Phase Equilib.* **289**, 156 (2010).
- ⁵⁹E. J. W. Wensink, A. C. Hoffmann, P. J. van Maaren, and D. van der Spoel, *J. Chem. Phys.* **119**, 7308 (2003).
- ⁶⁰H. Tanaka and K. E. Gubbins, *J. Chem. Phys.* **97**, 2626 (1992).
- ⁶¹J. A. Batista da Silva, F. G. B. Moreira, V. M. Leite dos Santos, and R. L. Longo, *Phys. Chem. Chem. Phys.* **13**, 6452 (2011).
- ⁶²G. Kaminski and W. L. Jorgensen, *J. Phys. Chem.* **100**, 18010 (1996).
- ⁶³T. A. Pascal, S.-T. Lin, and W. A. Goddard III, *Phys. Chem. Chem. Phys.* **13**, 169 (2011).
- ⁶⁴D. Gonzalez-Salgado and C. Vega, *J. Chem. Phys.* **132**, 094505 (2010).
- ⁶⁵D. Gonzalez-Salgado, A. Dopazo-Paz, P. Gomez-Alvarez, J. M. Miguez, and C. Vega, *J. Phys. Chem. B* **115**, 3522 (2011).
- ⁶⁶B. Hess, C. Kutzner, D. van der Spoel, and E. Lindahl, *J. Chem. Theory Comput.* **4**, 435 (2008).
- ⁶⁷C. Caccamo, *Phys. Rep.* **274**, 1 (1996).
- ⁶⁸P. H. Van Konynenburg and R. L. Scott, *Philos. Trans. R. Soc. London, Ser. A* **298**, 495 (1980).
- ⁶⁹D. G. Archer and R. W. Carter, *J. Phys. Chem. B* **104**, 8563 (2000).
- ⁷⁰R. W. Carter and D. G. Archer, *Phys. Chem. Chem. Phys.* **2**, 5138 (2000).
- ⁷¹A. R. Bazaev, I. M. Abdulagatov, J. W. Magee, E. A. Bazaev, A. E. Ramazanov, and A. A. Abdurashidova, *Int. J. Thermophys.* **25**, 805 (2004).
- ⁷²A. R. Bazaev, E. A. Bazaev, and A. A. Abdurashidova, *High Temp.* **42**, 895 (2004).
- ⁷³E. A. Bazaev, A. R. Bazaev, and A. A. Abdurashidova, *High Temp.* **47**, 195 (2009).
- ⁷⁴A. I. Abdulagatov, G. V. Stepanov, and I. M. Abdulagatov, *High Temp.* **45**, 85 (2007).
- ⁷⁵E. G. Strelakova, D. Corradini, M. G. Mazza, S. V. Buldyrev, P. Gallo, G. Franzese, and H. E. Stanley, *J. Biol. Phys.* **38**, 97 (2012).
- ⁷⁶E. G. Strelakova, M. G. Mazza, H. E. Stanley, and G. Franzese, *Phys. Rev. Lett.* **106**, 145701 (2011).
- ⁷⁷E. G. Strelakova, J. Luo, H. E. Stanley, G. Franzese, and S. V. Buldyrev, *Phys. Rev. Lett.* **109**, 105701 (2012).
- ⁷⁸P. Gallo and M. Rovere, *Phys. Rev. E* **76**, 061202 (2007).
- ⁷⁹A. Taschin, R. Cucini, P. Bartolini, and R. Torre, *EPL* **92**, 26005 (2010).
- ⁸⁰G. Wada and S. Umeda, *Bull. Chem. Soc. Jpn.* **35**, 646 (1962).
- ⁸¹S. Chatterjee, H. S. Ashbaugh, and P. G. Debenedetti, *J. Chem. Phys.* **123**, 164503 (2005).
- ⁸²S. V. Buldyrev, P. Kumar, P. G. Debenedetti, P. J. Rossky, and H. E. Stanley, *Proc. Natl. Acad. Sci. U.S.A.* **104**, 20177 (2007); Z. Su, S. V. Buldyrev, P. G. Debenedetti, P. J. Rossky, and H. E. Stanley, *J. Chem. Phys.* **136**, 044511 (2012); J. R. Dowdle, S. V. Buldyrev, H. E. Stanley, P. G. Debenedetti, and P. J. Rossky, "Temperature and length scale dependence of solvophobic solvation in a single-site water-like liquid," *J. Chem. Phys.* (submitted); S. Sharma, S. K. Kumar, C. A. Angell, S. V. Buldyrev, P. G. Debenedetti, P. J. Rossky, and H. E. Stanley, "A coarse-grained protein-like model with explicit solvent," *J. Chem. Phys.* (submitted).
- ⁸³A. K. Soper and M. A. Ricci, *Phys. Rev. Lett.* **84**, 2881 (2000).
- ⁸⁴R. Mancinelli, A. Botti, F. Bruni, M. A. Ricci, and A. K. Soper, *J. Phys. Chem. B* **111**, 13570 (2007).
- ⁸⁵D. Corradini, M. Rovere, and P. Gallo, *J. Phys. Chem. B* **115**, 1461 (2011).
- ⁸⁶P. Gallo, D. Corradini, and M. Rovere, *Phys. Chem. Chem. Phys.* **13**, 19814 (2011).
- ⁸⁷M. A. Ricci, F. Bruni, P. Gallo, M. Rovere, and A. K. Soper, *J. Phys. Condens. Matter* **12**, A345 (2000).
- ⁸⁸L. Dougan, R. Hargreaves, S. P. Bates, J. L. Finney, V. Réat, A. K. Soper, and J. Crain, *J. Chem. Phys.* **122**, 174514 (2005).
- ⁸⁹V. V. Vasisht, S. Saw, and S. Sastry, *Nat. Phys.* **7**, 549 (2011).
- ⁹⁰N. Micali, S. Trusso, C. Vasi, D. Blaudez, and F. Mallamace, *Phys. Rev. E* **54**, 1720 (1996).
- ⁹¹A. K. Soper and J. L. Finney, *Phys. Rev. Lett.* **71**, 4346 (1993).
- ⁹²K. Miyata and H. Kanno, *J. Mol. Liq.* **119**, 189 (2005).